Molecular Microbiology (2009) 71(1), 172–184 ■
doi:10.1111/j.1365-2958.2008.06520.x
First published online 6 November 2008

Aspergillus nidulans FlbE is an upstream developmental activator of conidiation functionally associated with the putative transcription factor FlbB

Aitor Garzia,[1] Oier Etxebeste,[1,2] Erika Herrero-Garcia,[3] Reinhard Fischer,[4] Eduardo A. Espeso[3] and Unai Ugalde[1]*

[1]*Department of Applied Chemistry, Faculty of Chemistry, University of the Basque Country, San Sebastian 20018 San Sebastian, Spain.*
[2]*CIC nanoGUNE, P° Mikeletegi 56, 301, 20009, San Sebastian, Spain.*
[3]*Departamento Microbiología Molecular, Centro de Investigaciones Biológicas (CSIC), Ramiro de Maeztu, 9, 28040 Madrid, Spain.*
[4]*Institute for Applied Biosciences, Department of Applied Microbiology, University of Karlsruhe, Hertzstrasse 16, D-76187 Karlsruhe, Germany.*

Summary

Aspergillus nidulans **switches from vegetative growth to conidiation when aerial hyphae make contact with the atmosphere, or are subjected to specific environmental stress. The activation of the central conidiation pathway led by the transcription factor *brlA* is a critical milestone in this morphogenetic transition. A number of upstream developmental activators (*UDA*s), expressed in vegetative cells, are required for this process to occur in conjunction with cessation of vegetative growth. Mutants affected in these factors remain aconidial (*fluffy*) with low *brlA* expression levels (*flb*). In this report, we describe FlbE as a *UDA* containing two conserved but hitherto uncharacterized domains, which functions in close association with putative transcription factor FlbB. Both *UDA*s are functionally interdependent, and colocalize at the hypha tip in an actin cytoskeleton-dependent manner. Moreover, bimolecular fluorescence studies show that they physically interact *in vivo*. These findings add evidence in favour of the existence of a signalling complex at or near the Spitzenkörper as an important part of the machinery controlling the morphogenetic transition between vegetative growth and conidiation.**

Accepted 21 October, 2008. *For correspondence. E-mail unaiona.ugalde@ehu.es; Tel. (+34) 943018180; Fax (+34) 943015270.

Introduction

Asexual development in *Aspergillus nidulans* involves the formation of specialized multicellular structures called conidiophores, each bearing large numbers of uninucleate propagules named conidia (Adams *et al*., 1998). Conidiophore development is controlled through a central regulatory pathway which is initiated with the activation of the transcription factor (TF) *brlA* (for a current review see Fischer and Kües, 2006). A variety of stimuli which are generally considered incompatible with polar cell growth, such as the emergence of hyphae to the atmosphere, nutrient depletion or osmotic stress, can trigger the process (Chang and Timberlake, 1993; Adams *et al*., 1998).

External stimuli are transduced into signals which are then processed to activate the central regulatory pathway via *brlA*. Some factors involved in this process have been identified and are collectively termed upstream developmental activators, *UDA*s (Yu *et al*., 2006). Mutations in *fluG* or any one of the genes termed *flbA–E* results in a *fluffy* (aconidial) phenotype with low levels of *brlA* expression (fluffy with low *brlA* expression = *flb*; Lee and Adams, 1994a; Wieser *et al*., 1994; Wieser and Adams, 1995). The FluG factor is required for the synthesis of a low-molecular-weight extracelular signalling molecule believed to accumulate in aerial hyphae (Lee and Adams, 1994b). *flbA* codes for a regulator of G protein signalling which inhibits vegetative growth signalling mediated by FadA, a Gα protein (Lee and Adams, 1994a; Yu *et al*., 1996; Yu, 2006). FlbD, FlbB and FlbC are potential TFs (Wieser and Adams, 1995; Adams *et al*., 1998; Etxebeste *et al*., 2008), and FlbE has not been characterized in depth. The mode of action of Flb factors in conidiation induction remains as yet unclear, although it has been established that they act in concert, and all are required to produce a second diffusible signal that is required for *brlA* activation (Yu *et al*., 2006).

In a previous paper, we described *flbB* as a gene coding for a bZIP type TF located at the hyphal apex and the apical nucleus (Etxebeste *et al*., 2008). In this work we characterize *flbE*, one of the least known *flb* gene family members. It codes for a small protein containing several

functionally significant domains. FlbE colocalizes and physically interacts with FlbB at the tip of vegetative hyphae, and both are mutually interdependent for proper localization and function.

The combined evidence supports the view that FlbE and FlbB form part of an early signalling complex situated at or in the vicinity of the Spitzenkörper (Girbardt, 1957), suggesting that this apical body could perform signalling functions other than those strictly involving the maintenance of polar tip extension.

Results

Isolation of flbE

In order to study the fluG signal transduction pathway, we isolated a collection of mutants with a fluffy growth phenotype. Aconidial mutants, obtained with nitrosoguanidine and UV mutagenesis, were screened for defects in extracellular conidiation signal synthesis by selecting colonies which conidiated when in contact with the wild-type reference strain FGSC26 (Lee and Adams, 1994b; see Table 1). The selected strains were then placed in contact with a *fluG* strain, and those that induced conidiation at the contact zone were chosen for further work (four isolates). Thus, the four mutants were defective in a second extracellular signal acting downstream of the FluG signal. Classical genetic analysis showed that three of the strains contained allelic mutations mapping at the *flbB* locus (Etxebeste *et al*., 2008).

The fourth aconidial mutant (strain BD13) contained a mutation which was not allelic to FlbB, in spite of its strikingly similar aconidial phenotype (see below). Diploid analysis using strains FGSCA68 (Kafer, 1965), FGSCA283 and GR5 (Waring *et al*., 1989) (see Table 1) as partners showed that the mutation at strain BD13 was located in chromosome VIII and was recessive (results not shown). To identify the affected gene, a genomic library cloned into the self-replicating pRG3/AMA1/NotI plasmid, obtained from the Fungal Genetics Stock Center (Osherov *et al*., 2000), was used in transformation to complement the aconidial mutation following the same procedure for the characterization of *flbB* mutants (Etxebeste *et al*., 2008). Strain BD13 was crossed with strain MAD782 yielding strain BD101, additionally carrying the selectable auxotrophic markers *pyrG89* and *argB2*, the former being required for the maintenance of the autoreplicative plasmid. Strain BD101 was transformed with the genomic library and several conidiating transformants were selected. From these transformants four different plasmids were isolated and verified in subsequent transformations for reversion of the aconidial phenotype of strain BD101. The flanking DNA sequences of the genomic DNA inserts at these plasmids were sequenced and compared with the genomic database accessible at the Broad Institute webpage (http://www.broad.mit.edu/annotation/genome/aspergillus_group/MultiHome.html). All fragments contained genes *AN0720.3*, *AN0721.3* and *AN0722.3*, from contig 11 mapped at chromosome VIII. Selective digestion of the fragments allowed for the generation of plasmids separately containing single-gene fragments (see Fig. S1). Transformation of these plasmids revealed that only those containing gene *AN0721.3* complemented the mutant defect. This locus was sequenced from strains BD101 and BD13 identifying a substitution of a CG pair (position 58 from the putative ATG) by a thymidine. This mutation caused a frameshift at residue 20 of the predicted amino acid sequence.

AN0721.3 was previously identified as *flbE*, a member of the upstream developmental pathway leading to the activation of *brlA* expression, and conidiation. Several mutants of this gene had been isolated in a chemical mutagenesis screen which yielded a *fluffy* aconidial phenotype (Yu *et al*., 2006 and references therein). This phenotype was further confirmed in this study by construction of a null allele of *flbE* (Fig. S1) in which a *brlA* transcript was absent (Fig. 6B).

FlbE is a protein specific to filamentous fungi, with unknown conserved domains

Genomic and cDNA versions of *flbE* were amplified and sequenced using specific primers, resulting in sequences identical to those published in the Broad Institute database. The ORF of *flbE* consists of 682 bp divided into two exons by a 73 nt intron (not shown). The predicted FlbE protein has 202 amino acids with an estimated molecular mass of 23.1 kDa and an isoelectric point of 4.28. Searches at the Pfam database did not provide any known conserved functional domains.

Wide-ranging searches in other genomic DNA and protein databases using the BLASTP programs showed putative orthologues in other *Aspergillus* species as *A. terreus*, *A. fumigatus*, *A. clavatus*, and the closely related *Neosartorya fischeri*, as well as in other filamentous fungi such as *Phaeosphaeria nodorum*, among others (Fig. 1). However, no homologues were found in genomes from yeast-like fungi or higher eukaryotes. Alignments of the most similar protein sequences to FlbE revealed the presence of two conserved regions (A and B; Fig. 1) with an elevated content of hydrophobic residues, separated by a non-conserved region, which we designated as a 'linker'. The C-terminal tail of the protein contiguous to the B region contained a segment significantly enriched with acidic residues.

The mutation found in strain BD13, now designated as *flbE001* (Fig. 1), caused an early truncation of the FlbE protein, which congruently resulted in a phenotype indis-

Table 1. *Aspergillus nidulans* strains used in this study.

Strain	Genotype	Source
FGSCA4	Wild type (*veA*$^{+}$)	Polley and Caddick (1996)
FGSC26	*biA1; veA1*	Kafer (1965)
FGSC A68	*suA1adE20; yA2; adE20; acrA1; phenA2; pyroA4; lysB5; sB3; nicB8; riboB2; veA1*	Kafer (1965)
FGSC A283	*suA1adE20; yA2; adE20; acrA1; galA1; pyroA4 (ssb*$^{+}$*); facA303; sB3; nicB8; riboB2; veA1*	Fungal Genetics Stock Center
TTA127.4	*ΔfluG::trpC; pabaA1; yA2; veA1*	Lee and Adams (1994b)
RMSO11	*ΔargB::trpCΔB; trpC801; pabaA1; yA2; veA1*	Stringer *et al.* (1991)
GR5	*pyrG89; pyroA4; wA; veA1*	Waring *et al.* (1989)
MAD782	*pyrG89; pabaA1; biA1; yA2; veA1*	Eduardo Espeso (CIB-CSIC, Madrid, Spain)
TN02A3	*ΔnkuA::argB; argB2; pyrG89; pyroA4; veA1*	Nayak *et al.* (2006)
TN02A21	*ΔnkuA::argB; argB2; riboB2; pyroA4; veA1*	Nayak *et al.* (2006)
TN02A25	*ΔnkuA::argB; argB2; pyrG89; riboB2; pabaB22; veA1*	Nayak *et al.* (2006)
WIM126	*pabaA1; yA2; veA*$^{+}$	Butnick *et al.* (1984)
flbE001 (BD13)	*flbE001; biA1, veA1*	This study
flbE::GFP	*ΔnkuA::argB; argB2; flbE::gfp/pyrG; pyrG89; pyroA4; veA1*	This study
flbE101	*flbE002; ΔnkuA::argB; argB2; flbE::gfp/pyrG; pyrG89; pyroA4; veA1*	This study
flbE102	*flbE003; ΔnkuA::argB; argB2; flbE::gfp/pyrG; pyrG89; pyroA4; veA1*	This study
flbE103	*flbE004; ΔnkuA::argB; argB2; flbE::gfp/pyrG; pyrG89; pyroA4; veA1*	This study
BD101	*flbE001; argB2; pyrG89; yA2; pabaA1; VeA1*	This study
BD142	*ΔnkuA::argB; argB2; ΔflbE::pyrG; pyrG89; pyroA4; veA1*	This study
BD143	*ΔnkuA::argB; argB2; ΔflbB::pyrG; pyrG89; pyroA4; veA1*	Etxebeste *et al.* (2008)
BD160	*ΔnkuA::argB; argB2; pyrG89; riboB2; pabaB22; pyroA4; veA1*	This study
BD162	*ΔflbE::pyrG; pyrG89; pabaA1, yA2; argB2*	This study
flbB::GFP (BD167)	*ΔnkuA:argB; argB2; flbB:gfp/pyrG; pyrG89; pyroA4; veA1*	Etxebeste *et al.* (2008)
BD178	*ΔnkuA::argB; argB2; pyrG89; ΔflbE::ribo riboB2; pabaB22; pyroA4; veA1*	This study
BD186	*ΔnkuA::argB; argB2; flbE::gfp/pyrG; pyrG89; pyroA4; veA1*	This study
BD176	*ΔnkuA::argB; argB2; flbB::gfp/pyrG89; ΔflbE::ribo; riboB2; pabaB22; pyroA4; veA1*	This study
BD177	*ΔnkuA::argB; argB2; pyrG89; ΔflbB::ribo riboB2; pabaB22; pyroA4; veA1*	This study
BD187	*ΔnkuA::argB; argB2; flbE::gfp/pyrG89; ΔflbB::ribo; riboB2; pabaB22; pyroA4; veA1*	This study
BD188	*ΔnkuA::argB; argB2; pyrG89; alcA(p)::pyroA*; pyroA4; veA1*	This study
BD189	*ΔnkuA::argB; argB2; pyrG89; alcA(p)::flbE::pyroA*; pyroA4; veA1*	This study
BD191	*ΔnkuA::argB; argB2; pyrG89; ΔflbE::ribo riboB2; pabaB22; alcA(p)::pyroA*; pyroA4; veA1*	This study
BD192	*ΔnkuA::argB; argB2; pyrG89; ΔflbE::ribo riboB2; pabaB22; alcA(p)::flbE::pyroA*; pyroA4; veA1*	This study
BD193	*ΔnkuA::argB; argB2; pyrG89; ΔflbE::ribo riboB2; pabaB22; alcA(p)::flbB::pyroA*; pyroA4; veA1*	This study
BD194	*ΔnkuA::argB; argB2; pyrG89; ΔflbB::ribo riboB2; pabaB22; alcA(p)::pyroA*; pyroA4; veA1*	This study
BD195	*ΔnkuA::argB; argB2; pyrG89; ΔflbB::ribo riboB2; pabaB22; alcA(p)::flbE::pyroA*; pyroA4; veA1*	This study
BD196	*ΔnkuA::argB; argB2; flbE::CR/pyroA; gfp::flbB; pyrG89; pyroA4; veA1*	This study
BD224	*ΔnkuA::argB; argB2; pyrG89; pyroA4; veA1; alcA::YFP*^{N}*::flbB::pyr-4;*	This study
BD225	*ΔnkuA::argB; argB2; pyrG89; pyroA4; veA1; alcA::YFP*^{C}*::flbE::pyr-4*	This study
BD226	*ΔnkuA::argB; argB2; pyrG89; pyroA4; veA1; alcA::YFP*^{N}*::flbB::pyr-4; alcA::YFP*^{C}*::flbE::pyroA*	This study

tinguishable from that of the null mutant. In addition, during the GFP tagging of FlbE (see below) three additional mutants were obtained through spontaneous amplification errors. The strains (*flbE101*, *102* and *103*) had aconidial phenotypes, and were subsequently characterized. Sequencing of the integrated construct showed that *flbE101* also contains an early truncation in FlbE, R10Stop (see Table 2). FlbE102 carries an amino acid substitution at position 120: S120P, and finally, FlbE103 contains an Ala to Val change at position 131 (A131V). One of the amino acid changes (*flbE102*: S120P) is located within the 'linker region'. In contrast with *flbE103*, *flbE102* does not affect a conserved residue (see alignment at Fig. 1), although it might alter the flexibility of the protein. This exerts complete loss of function in FlbE reflecting the functionality of a flexible 'linker' or the B

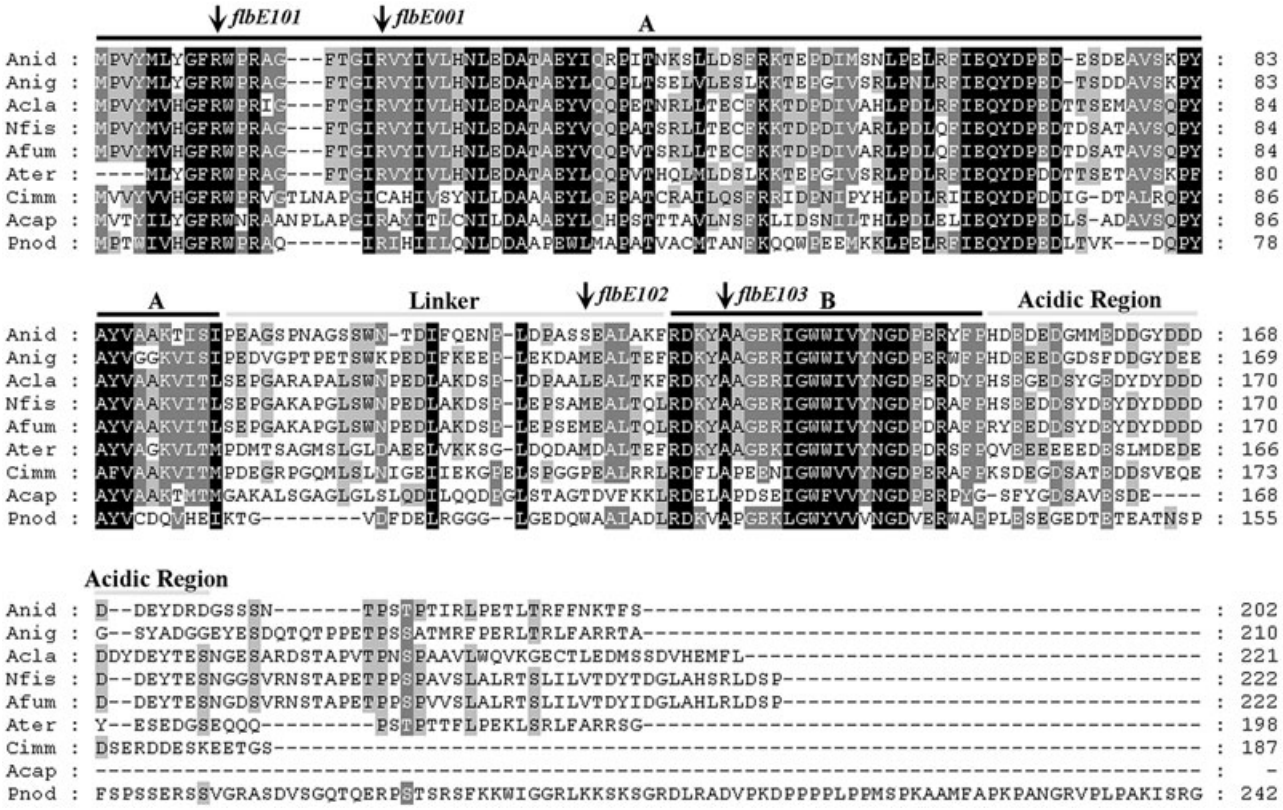

Fig. 1. General description of *flbE*. Alignment of putative FlbE homologues in different filamentous fungal species. Genedoc software was used (version 2.6.003; http://www.psc.edu/biomed/genedoc). Abbreviations: Anid, *A. nidulans*; Anig, *A. niger*; Acla, *A. clavatus*; Nfis, *N. fischeri*; Afum, *A. fumigatus*; Ater, *A. terreus*; Cimn, *Coccidioides immitis*; Acap, *Ajellomyces capsulata*; Pnod, *P. nodorum*.

region (Figs 2 and 3). The presence of the GFP tag in the construct allowed us to examine the implications of these mutations at the intracellular protein expression level, as well as localization (see below).

Phenotypic characterization of flbE *mutants*

In order to gain a better understanding of the role of FlbE in growth and morphogenesis, a full phenotypic characterization of all the mutants was undertaken, along with a reference strain that is wild type for conidial production (TN02A3). The experimental design incorporating carbon and nitrogen depletion (Skromne *et al*., 1995), and osmotic stress already described and previously used to characterize *flbB* mutants (Etxebeste *et al*., 2008) provided a useful benchmark for a comparative evaluation of the new mutants.

Table 2. Mutations characterized in this study.

Allele	DNA change(s)	Mutant protein	Changes in protein
flbE001	C58T;G59Δ	1-19+WSTSSCTT	R20W
flbE101	C27T;C28T	1-9	R10STOP
flbE102	T358C	1-202	S120P
flbE103	C391T	1-202	A131V

On complete or synthetic minimal medium (MMA), the strain expressing the GFP-tagged version of FlbE, allele *flbE::gfp*, displayed an identical phenotype to the untagged strain (not shown), demonstrating the functionality of the fusion protein. On the other hand, the different *flbE* mutant alleles, mentioned in the previous section, presented comparable phenotypes to that of the null *flbE* strain (not shown for *flbE001* and *flbE101*). This characteristic led us to conclude that all the mutant alleles causing early truncations or amino acid changes corresponded to loss-of-function mutations.

In surface cultures, all the loss-of-function mutants showed an aconidial phenotype in MMA (Fig. 2), while an 80% reduction in glucose provoked low levels of conidiation at the colony centre. An equivalent reduction in nitrogen source did not induce any appreciable phenotypic change. Under saline stress growth conditions (MMA supplemented with 0.6 M KCl), mutant colonies displayed conidiophores at the upper levels of a mainly *fluffy* mycelium. This response was indistinguishable from that observed in the null mutant of *flbB* studied earlier (Etxebeste *et al*., 2008; not shown).

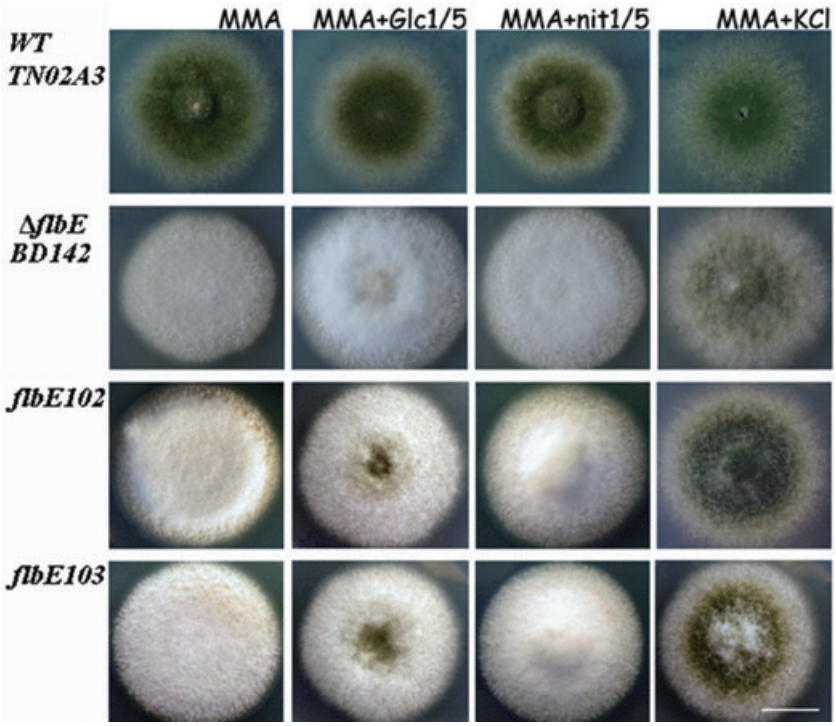

Fig. 2. *flbE* mutant characterization on solid media. Colony morphologies of wild-type (WT; TN02A3), Δ*flbE* (BD142), *flbE102* and *flbE103* strains grown on solid MMA, MMA with 0.4% glucose, MMA with reduced nitrate and MMA with 0.6 M KCl (see *Experimental procedures*) for 72 h are shown. Strains carrying mutant alleles *flbE001*, *flbE::gfp* or *flbE101* are not shown. *flbE001* and *flbE101* mutant strains, as predicted by causing early truncated proteins, showed similar *fluffy* colony morphology and sparse conidiation like the strain carrying the allele Δ*flbE*. *flbE::gfp* strain does not differ from a WT strain. Bar = 1 cm.

Under liquid culture conditions, transfer into carbon-free medium for 20 h resulted in the production of simplified conidiophores by both the wild-type strain (Skromne *et al*., 1995) and the mutant strains (indicated by black arrows in Fig. 3). In contrast, cells from mutant strains were of unusual small diameter (1.5 μm, as opposed to normal diameter of wild-type hyphae, 3 μm; Fig. 3). This feature was also found in the *flbB* mutant (Etxebeste *et al*., 2008).

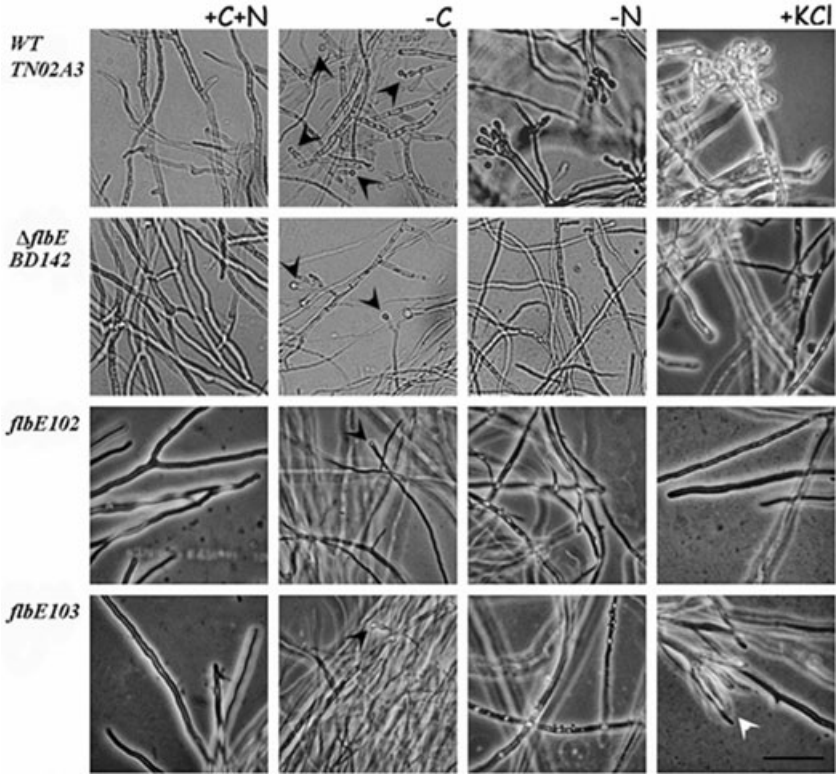

Fig. 3. Characterization of the *flbE* mutant strains in liquid media. Photographs of mycelia from wild-type (WT; TN02A3), Δ*flbE* (BD142), *flbE102* and *flbE103* strains after 18 h of culture in liquid MMA, followed by transfer to liquid MMA-glucose, MMA-nitrate or MMA plus 0.6 M KCl (buffered at pH = 6.5 with 0.05 M 2-[N-Morpholino]ethanosulphonic acid, MES) for a further 20 h (see *Experimental procedures*), are shown. Arrowheads indicate conidium-like structures. Strains carrying mutant alleles *flbE001*, *flbE::gfp* or *flbE101* are not shown. *flbE001* and *flbE101* mutant strains act like Δ*flbE* (no conidiophore differentiation) while *flbE::gfp* strain acts like the wild-type strain. Bar = 30 μm.

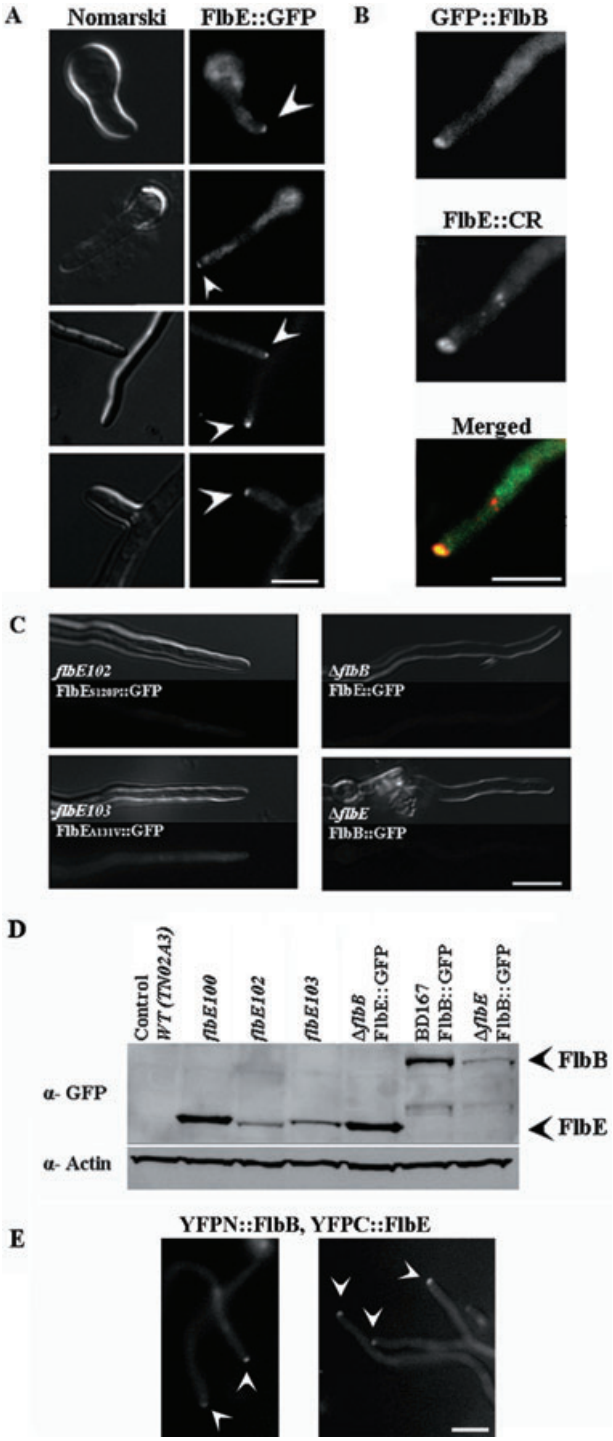

Fig. 4. Intracellular localization of FlbE (using strain *flbE::GFP*).
A. In static culture in liquid MMA, the FlbE::GFP protein accumulates since germling during vegetative growth (different structures characteristic of the vegetative growth are shown) at the hyphal tip (arrowheads). Fluorescence at the cytoplasm is also visible, although in these images the contrast has been intentionally modified.
B. GFP::FlbB and FlbE::CherryRed (BD196) proteins colocalized at the hyphal tip during vegetative growth.
C. Intracellular localization of aconidial mutants *flbE102* and *flbE103* and localization of FlbB and FlbE proteins in a null mutant background of the other (BD176 and BD187 respectively).
D. Western blot analyses, using anti-GFP and anti-actin primary antibodies.
E. BiFC analysis of FlbB and FlbE. In strain expressing YFP^N::FlbB and YFP^C::FlbE, yellow fluorescence was detected at the hyphal tip (arrowheads). Bar = 10 μm.

In medium without nitrogen, the wild-type strain developed complex conidiophores (Skromne *et al.*, 1995), while the Δ*flbE* and the rest of the loss-of-function mutant alleles remained vegetative, showing considerable levels of vacuolation and autolysis, as observed with fluorescein as a vital stain (not shown). Salt stress (KCl, 0.6 M) induced conidiation in the wild-type strain, while the Δ*flbE* and *flbE*$^-$ strains remained aconidial, with the exception of *flbE103*, which produced defective conidiophores with elongated metulae (indicated by white arrows in Fig. 3).

The combined results of the phenotypic analysis indicate that the null and mutant alleles of *flbE* do not show a differential phenotypic response under different culture conditions, and moreover, that these resemble those previously described for *flbB* mutants (Etxebeste *et al.*, 2008). This was interpreted as an indication that both FlbB and FlbE may be functionally related.

FlbE is associated to FlbB at the hyphal tip in vegetative cells

In order to study the cellular location of FlbE, a strain expressing it with a green fluorescent protein (GFP) tag at the C-terminus (FlbE::GFP) was generated (*flbE::gfp*). Static liquid cultures of the strain revealed that FlbE::GFP accumulated at the hyphal tip on germination, and this localization remained unaltered in leading hyphae and branches at all times (Fig. 4A). This apical localization pattern was indistinguishable from that of FlbB::GFP-labelled strains (BD167) described in an earlier study (Etxebeste *et al.*, 2008). This possible colocalization was confirmed by the analysis of a strain expressing both GFP::FlbB and FlbE::CherryRed (Fig. 4B).

The aconidial mutants *flbE102* and *flbE103*, which expressed GFP-labelled defective proteins, showed no fluorescence at the hyphal tip (Fig. 4C). Western blot analysis further confirmed that these mutant proteins were expressed at lower levels (Fig. 4D, lanes 3 and 4). Therefore, the aconidial phenotype of these mutant strains was assigned to mislocalization of FlbE::GFP from the tip of the cell, possibly followed by partial degradation.

Given that FlbE and FlbB colocalized at the hyphal tip, the possibility that they may interact physically was considered, and this, in turn, could entail that one factor could be required for the correct localization of the other. Thus, the localization of either protein was observed in a null

mutant background of the other. The results in Fig. 4C show that apical accumulation of FlbB::GFP fluorescence is lost in an *flbE* background. When FlbE localization was studied in an *flbB* background, no fluorescence was observed along the hyphae. In order to determine if loss of fluorescence accumulation was a result of protein degradation, extracts from the above-mentioned strains were analysed by Western blot showing that the protein titre of FlbB was significantly lower in the absence of FlbE (Fig. 4D, lane 7). In addition, a lower-molecular-weight band indicated the presence of a truncated form of the protein, presumably lacking the bZIP region. Conversely, FlbE protein levels remain unaltered in an *flbB* background (Fig. 4D, lane 5). These results indicate that FlbB and FlbE are interdependent for proper cell localization, to the extent that FlbB stability is affected in the absence of a functional form of FlbE.

The possible physical interaction between FlbB and FlbE was evaluated *in vivo* by the BiFC system (Takeshita *et al*., 2008). The N-terminal half of yellow fluorescent protein (YFP^N) was fused to the N-terminus part of FlbB, and the C-terminal half of YFP (YFP^C) to the N-terminus part of FlbE, both of them under the control of the inducible *alcA* promoter. In the strains expressing only YFP^N::FlbB or YFP^C::FlbE, no fluorescence was detected (not shown). Coexpression of YFP^N::FlbB and YFP^C::FlbE showed reconstituted YFP signal at the hyphal tip (Fig. 4E). This apical localization pattern was in agreement with that observed in the double-tagged strain (Fig. 4B).

FlbE and FlbB apical localization depends on the F-actin cytoskeleton

Since both FlbE and FlbB presented an apical localization pattern, its dependence on cytoskeletal elements such as tubulin dimers (Horio and Oakley, 2005; Steinberg, 2007a) or F-actin cytoskeletons (Steinberg, 2007a,b) was considered (Fig. 5).

To study the dependence of FlbE and FlbB localization on microtubules or actin microfilament stability, we used benomyl and latrunculin B following our standardized protocols (Araújo-Bazán *et al*., 2008; Taheri-Talesh *et al*., 2008). Addition of benomyl barely affected the apical localization of either FlbE or FlbB although the tip morphology was clearly altered through disturbance of the tubulin cytoskeleton, as previously reported (Upshall *et al*., 1977) (Fig. 5B). Conversely, addition of latrunculin B caused mislocalization of both FlbB and FlbE (Fig. 5C), which could be reversed 5 min after transferring mycelia to MMA (not shown). These results clearly indicate that both proteins require the F-actin cytoskeleton, although the precise nature of this relationship remains to be specified. We also observed mislocalization of both FlbE and FlbB in a medium containing sodium azide and sodium fluoride (not shown), suggesting that this localization pattern is generated by an active transport mechanism.

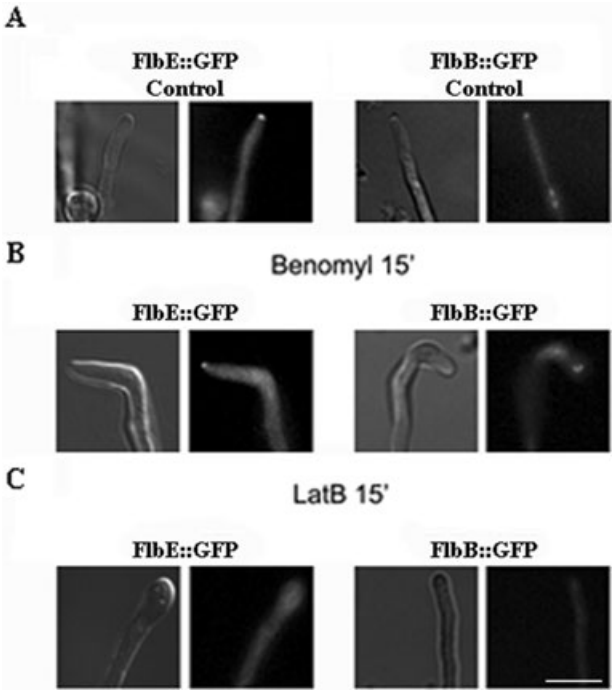

Fig. 5. Effect of cytoskeleton destabilizing drugs on FlbE and FlbB localization (A) control medium without any added compound; (B) in the presence of 3 μg ml^{-1} of benomyl; and (C) in the presence of latrunculin B at 100 μM. Bar = 10 μm.

flbE *is expressed throughout the life cycle*

Northern blot experiments were performed to analyse the expression levels of *flbE* throughout the life cycle of *A. nidulans*, and to analyse a hypothetical interdependence of *flbE* and *flbB* transcriptional profiles.

The expression profile of *flbE* shown in Fig. 6A indicates that it is present at all the stages of the life cycle. The transcriptional activation of *brlA*, which marks the initiation of conidiation, did not alter the expression profile of *flbE*, by contrast with the downregulation observed in *flbB* expression (Fig. 6A; Etxebeste *et al*., 2008). In agreement with the previous result, *flbE* expression was at most slightly downregulated in an *flbB* background (Fig. 6B). In addition, FlbE was not strictly required for the expression of *flbB* (Fig. 6B), although lower levels of *flbB* transcription were observed in the Δ*flbE* background which might explain the lower levels of FlbB protein found (Fig. 4E). The expression levels observed in strains carrying either the *veA* wild-type allele (WIM126) or the mutant *veA1* allele (TN02A3) were comparable (Fig. 6A and B respectively). Thus, it would appear that *flbE*

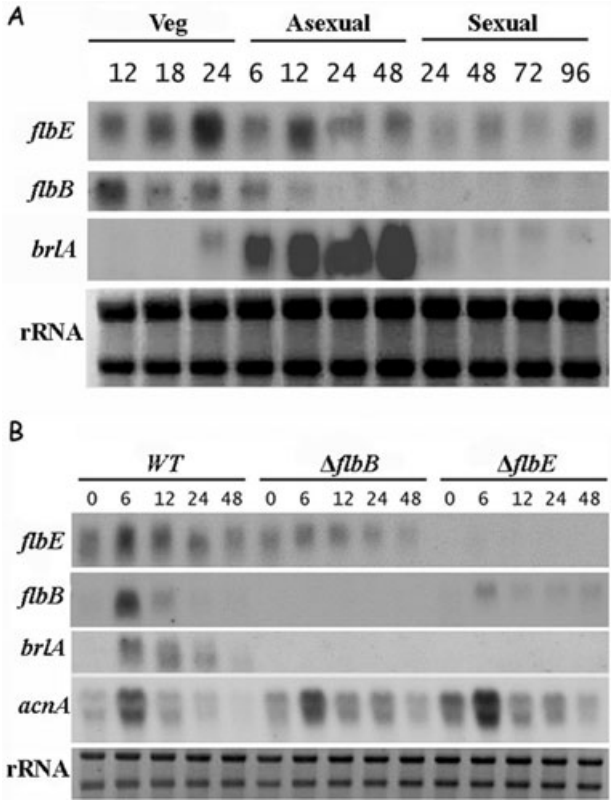

Fig. 6. *flbE*, *flbB*, *brlA* and *acnA* (actin, loading control) mRNA expression.
A. During the *A. nidulans* life cycle in a wild-type *veA* genetic background (strain WIN126). Numbers indicate the time (hours) of incubation in liquid MMA plus glucose, corresponding to vegetative growth (Veg), or under conditions inducing asexual (Asexual) or sexual development (Sexual) respectively (see *Experimental procedures*). Note that *flbE* is expressed during the life cycle, and *flbB* and *brlA* are expressed as previously described (Etxebeste *et al*., 2008).
B. *flbE*, *flbB*, *acnA* and *brlA* mRNA expression levels at different times during vegetative (0) and asexual development (6, 12, 24 and 48 h), in the *flbE* and *flbB* null mutant strains compared with the wild-type *veA1* (WT) strain. *acnA* expression levels vary throughout the life cycle, but experiments with different strains show comparable levels of expression for each life cycle stage.

expression is not under the control of the upstream regulator VeA, mediating light-dependent conidiation. The combined results indicate that *flbE* is expressed at relatively constant levels throughout the life cycle and that this pattern is independent of the expression pattern of *flbB*.

FlbE acts along the FluG pathway at the same level as FlbB

In order to position *flbE* in relation to functionally linked *flbB*, the phenotype of overexpression of *flbB* was analysed in wild-type, Δ*flbE* and Δ*flbB* backgrounds. In addition, overexpression of *flbB* in a Δ*flbE* background was also evaluated. *flbE* overexpression could not overcome the aconidial phenotype imposed by Δ*flbB*, and an identical result was observed when *flbB* was overexpressed in a Δ*flbE* background (Fig. 7). This would place both factors at the same functional level as upstream developmental regulators and confirms the indications shown earlier that they are intimately associated. Thus, FlbE and FlbB have to be considered as acting at the same level in the *UDA* signalling pathway, immediately before the BrlA TF.

An earlier study indicated that FlbB activity results in the production of an extracellular signal acting downstream of the FluG signal (Etxebeste *et al*., 2008). This feature is common to all *flb*(*A–E*) mutants (Wieser *et al*., 1994). All the *flbE* mutants described in this report follow the above-mentioned pattern of extracellular complementation. Moreover, *flbE* and *flbB* mutants were unable to transfer any extracellular signal that complemented their respective aconidial phenotypes (Fig. 8). This observation further supports the view that FlbB and FlbE act at the same step in the conidiation induction pathway, in coherence with the rest of results obtained in this study.

Discussion

In this article, the FluG-dependent upstream developmental pathway member FlbE has been characterized, espe-

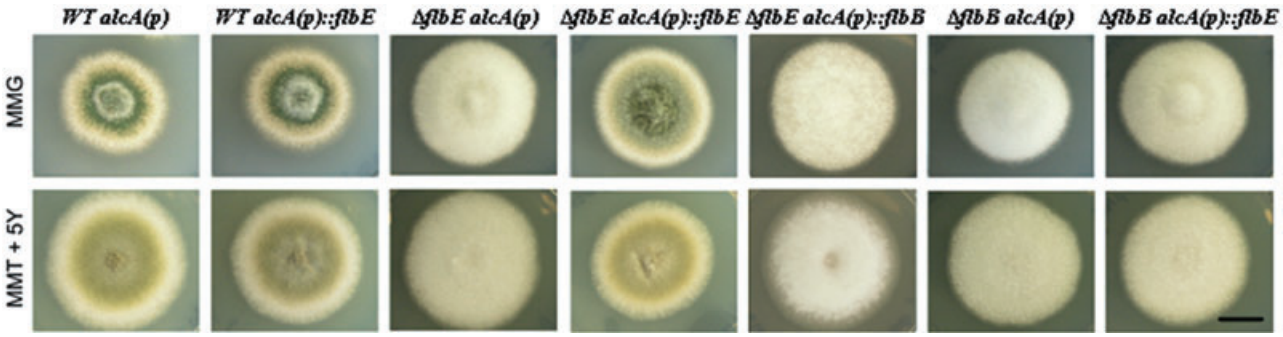

Fig. 7. Overexpression experiments in different genetic backgrounds. *flbE* overexpression does not affect wild-type conidiation phenotype. Photographs of the colonies of controls and overexpression strains grown on MMA plus glucose (MMG; non-inducing) and MMA plus yeast extract (MMT + 5Y; threonine-inducing *alcA* promoter, with 5 g l^{-1} yeast extract enhancing growth) for 72 h are shown. Overexpression of *flbE* and *flbB* does not suppress Δ*flbB* and Δ*flbE* mutations respectively. Bar = 1 cm.

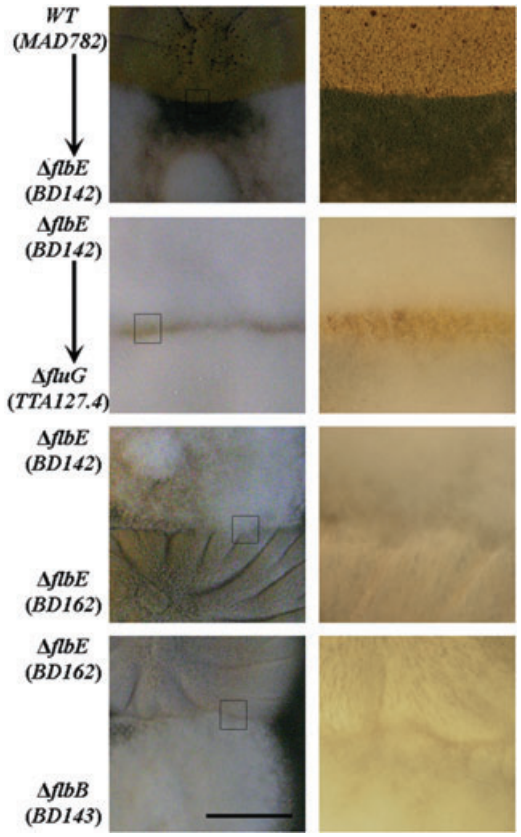

Fig. 8. Extracellular complementation experiments for conidiation induction. The Δ*flbE* (BD142) mutant conidiates in the contact zone with a wild-type strain (MAD782) and acts as a donor of a signalling molecule to a Δ*fluG* strain (TTA127.4). Absence of extracellular complementation for the signalling molecule is observed at the contact region between Δ*flbE* (BD142) and Δ*flbB* (BD143) strains. There is no complementation between two Δ*flbE* null mutant strains (BD142 and BD162). The pictures on the right side are enlargements of the contact zone. The yellow band in the second picture from the top represents yellow conidiospores. Bar = 1 cm for the left and 10× magnification of left panel for the right pictures.

cially focusing on its association with the bZIP type factor FlbB. This potential TF has been recently reported to localize to the apical nucleus as well as the hyphal tip (Etxebeste *et al*., 2008). This latter feature led us to propose that FlbB could be part of a conidiation signalling complex colocalized with the polar growth machinery at the hyphal tip dome (Etxebeste *et al*., 2008; Taheri-Talesh *et al*., 2008). The present work defines the functional interdependence between FlbE and FlbB, and provides new evidence in support of the apical complex hypothesis.

Epistasis analysis carried out in previous works placed *flbE* in the same pathway as *flbB* and *flbD* (Wieser *et al*., 1994). Overexpression assays further suggested that FlbE acted first in the sequence FlbE→FlbD→FlbB (Wieser and Adams, 1995). In later work, FlbE was described as a protein with unknown domains with an assigned role as repressor of *sfgA* or of hypothetical SAR genes (SfgA-Activated Repressors of conidiation; Seo *et al*., 2006).

Various lines of evidence obtained in this study confirm a functional interdependence between FlbB and FlbE. The indistinguishable phenotypes of *flbE* and *flbB* mutants under all tested conditions include blocked synthesis of the same diffusible second signalling factor necessary for conidiation (acting downstream from the FluG-dependent diffusible factor). In addition, overexpression of *flbB* does not result in suppression of the Δ*flbE* aconidial phenotype or vice versa. These results strongly indicate that both factors act at the same step and are interdependent. In addition, colocalization of both factors at the hypha tip, the dependence of FlbB localization and stability on the correct expression of FlbE, and evidence of physical interaction add further proof that both factors are part of a functional complex.

Despite the proven relation with FlbB, a precise role for FlbE cannot be established, although the fact that FlbE deletion results in mislocalization and partial degradation of FlbB suggests that one of the possible functions of FlbE may be to secure adequate localization and function of FlbB at or near the Spitzenkörper. This would explain the above-mentioned coincidence in phenotype of null mutants of both factors. The latrunculin B studies indicate a dependence on the actin cytoskeleton for proper localization, which should be clarified at the molecular level in later investigations. In this regard, it is interesting to note that mutation A131V is effective in causing FlbE mislocalization. This could be considered as preliminary evidence in favour of region B of the protein (see Fig. 1) playing a role in actin-dependent apical localization. On the other hand, mutation S120P located at the linker region, might interfere with the spatial organization of the conserved A and B regions in the protein or prevent the interaction with another factor implicated in a putative complex. Whether FlbB localization dependence with respect to FlbE also corresponds to domains in regions A or B (Fig. 1) requires further detailed examination.

The presence of FlbB at the hyphal tip may correspond to a particular form of the protein which, upon stimulus-related modifications, could be relocated to the nucleus in a new form which triggers a new morphogenetic programme. The truncated form of FlbB shown in Fig. 4D would indicate that the protein is cleaved into at least two fragments, one presumably carrying the DNA-binding domain at the N-terminal half of the protein, and the observed truncated form (Fig. 4D) containing the C-terminal half, which was earlier ascribed a *trans*-activation capacity (Etxebeste *et al*., 2008). A more detailed examination of the post-translational modifications taking place in FlbB with relation to its cellular distri-

Table 3 Oligonucleotides used in this study.

Oligo	Sequence (5′–3′)	Objective
pRG3up	GAA TTC GAG CTC GGT ACC	Sequencing pRG3 insert flanking regions
pRG3 down	AAG CTT GCA TGC GCG GCC	Sequencing pRG3 insert flanking regions
AN0721-1	CGC AAA TGC AGA CAA GG	*flbE* sequencing
AN0721-2	CCA TCT TGT CTG ATG GCC	*flbE* sequencing
flbE-GSP1	GCT GCA AGG GGT CGC AGA ACG AAC C	*flbE*::*gfp/pyrG* or *flbE*::*CR/pyroA* obtaining
flbE-GSP1*	GGA ATC CGG GTC TAC ATC GTC TTG CAC AAC C	*flbE*::*gfp/pyrG* or *flbE*::*CR/pyroA* obtaining
flbE-GSP2	CGA AAA CGT TTT GTT GAA GAA TCG CGT TAA TGT CTC	*flbE*::*gfp/pyrG* or *flbE*::*CR/pyroA* obtaining
flbE-GSP3	TGA TTG CTG TAC GAG TTA TAT TAC GAC TGA TGA	*flbE*:: *gfp/pyrG* or *flbE*::*CR/pyroA* and Δ*flbE* obtaining
flbE-GSP4	GCT TAC CTG CTG GAT CTC CTG CCG GTA CTT AGG	*flbE*:: *gfp/pyrG* or *flbE*::*CR/pyroA* and Δ*flbE* obtaining
flbE-PP1	GCA ACA AAT TCG GCT GTT GGG CTC AGG	*gfp*::*flbE* and Δ*flbE* obtaining
flbE-PP2	CAT GGT AAG GCG ACG ACG GCC CTC	*gfp*::*flbE* and Δ*flbE* obtaining
flbE-GFP1	GAG ACA TTA ACG CGA TTC TTC AAC AAA ACG TTT TCG GGA GCT GGT GCA GGC GCT GGA GCC	*flbE*::*gfp/pyrG* or *flbE*::*CR/pyroA* obtaining
flbE-GFP2	TCA TCA GTC GTA ATA TAA CTC GTA CAG CAA TCA GTC TGA GAG GAG GCA CTG ATG CG	*flbE*:: *gfp/pyrG* or *flbE*::*CR/pyroA* and Δ*flbE* obtaining
flbE-SMP1	GAG GGC CGT CGT CGC CTT ACC ATG ACC GGT CGC CTC AAA CAA TGC TCT	Δ*flbE* obtaining
alcA(p) sens	GGG GTA CCG AAC TAG TGG ATC TGC GAT GC	5′ end of *alcA*(p)
alcA(p) antis	GCT CAG CTG GAA TTC CTG C	3′ end of *alcA*(p)
*flbE*over sens	GGA ATT CCA TGC CAG TCT ACA TGC TC	*flbE* overexpression 5′ amplification and *flbE* forward primer for probe
*flbE*over antis	GGA ATT CCG TAC AGC AAT CAC GAA AAC G	*flbE* overexpression 3′ amplification, *flbE* reverse primer for probe and double hybrid
*flbB*over sens	CGG GAT CCC GCC ATG ACT TCG ATC AGT AGT AGG	*flbB* overexpression 5′ amplification and *flbB* forward primer for probe
*flbB*over antis	GGA ATT CCT GTC AGG TCA TGA ATA CAT CG	*flbB* overexpression 3′ amplification and *flbB* reverse primer for probe
*flbE*cDNA1	GTC CAG ACT CAT TAC CAG CG	*flbE* cDNA 5′ amplification
*flbE*cDNA2	CAT TCC CAA TGT TTG GGG	*flbE* cDNA 3′ amplification
*flbB*cDNA1	GGT CGC ATT TCA ACC TCC	*flbB* cDNA 5′ amplification
*flbB*cDNA2	AGT AAA TGG GAA ATA AGG GC	*flbB* cDNA 3′ amplification
*brlA*probe sens	CCA TGC AGA TCA GCC CTC	*brlA* forward primer for probe
*brlA*probe antis	CGG AAT TCG TAA ACT GAA CGG TGC TC TGG	*brlA* reverse primer for probe
*acnA*probe sens	CGG AAT TCG ATC GGT ATG GGT CAG AAG G	*acnA* forward primer for probe
*acnA*probe antis	CGG AAT TCG ATG TTG CCG TAC AGA TCC	*acnA* reverse primer for probe
flbB-YFPsense	GGG GCG CGC CCA TGA CTT CGA TCA GTA GTA GGC C	*flbB* forward amplification for YFP
flbB-YFPantis	CCT TAA TTA AGG TTC AGG TTT ACC TGA TCC TGC	*flbB* reverse amplification for YFP
flbE-YFPsense	CGG CGC GCC CAT GCC AGT CTA CAT GCT CTA CG	*flbE* forward amplification for YFP
flbE-YFPantis	CCT TAA TTA AGG CCT CGC AAA TGC AGA CAA GG	*flbE* reverse amplification for YFP

bution and dynamics may clarify its relation with other *UDA* functions. The similar phenotypes displayed by mutations at other known Flb factors, such as FlbC and FlbD, suggest that these proteins may also take part of the newly found complex. Notably, the outlook emerging from the evidence presented is coherent with the control of a process which involves the cessation of growth at the tip, and the change of morphogenetic programmes necessarily involving gene expression changes at the nuclear level.

Given the implications of the results obtained in this study, the existence of a putative complex exerting control on the activation of alternative morphogenetic programmes at the hyphal tip is reinforced. Hence a new perspective appears to emerge on the Spitzenkörper, not only as a vesicle-delivery centre required for growth (Bartnicki-Garcia *et al*., 1995), but also as a signal-processing centre that integrates environmental and endogenous signals, and co-ordinates the machineries required to activate or suppress the different morphogenetic programmes.

Experimental procedures

Strains, media and culture conditions

The strains employed in this study are listed in Table 1 and oligonucleotides are listed in Table 3. Strains were cultured and crossed as previously described (Pontecorvo *et al*., 1953) using minimal medium (MMA) or complete medium (MCA; MMA + 5 g l^{-1} yeast extract), in solid or liquid form with the appropriate supplements. Nutrient depletion experiments were performed as described by Etxebeste *et al*. (2008) in solid and by Skromne *et al*. (1995) in liquid media.

Extracellular complementation experiments were conducted as described by Etxebeste *et al*. (2008), by point inoculation of two strains at a distance of 2 cm onto solid

medium in a Petri dish. After 3, 4 or 5 days, contact zones were observed and photographed with a binocular microscope (Nikon SMZ800).

Induction of sexual and asexual development (Aguirre, 1993; Law and Timberlake, 1980) and intracellular localization analysis (Peñalva, 2005; Bernreiter *et al*., 2007; Stinnett *et al*., 2007) were carried out as previously described by Etxebeste *et al*. (2008).

Cloning of flbE

The mutant strain BD101 (*biA1*, *argB2*, *pyrG89*), derived from BD13, was transformed, as described by Tilburn *et al*. (1983), with a wild-type gene library inserted in the self-replicating plasmid pRG3/AMA1/NotI (Osherov *et al*., 2000). The modifications on the protocol are described by Etxebeste *et al*. (2008). The plasmid was recovered from conidiating transformants using a Plant Genomic DNA isolation Kit (Sigma) and amplified in *Escherichia coli* (DH5). Direct sequencing of the insert using oligonucleotides pRG3up and pRG3down identified locus *AN0721.3* (Accession No. EAA65198), a gene previously identified as *flbE* (Yu *et al*., 2006), but whose characterization remained to be done. The ORF of the gene was amplified using oligonucleotides AN0721-1 and AN0721-2 (Table 3), and the mutation was determined by comparative sequencing of the amplified fragment from mutant and reference strain FGSC26 genomic DNAs. Aconidial transformants tagged with GFP were also sequenced with oligonucleotides AN0721-1 and AN0721-2 (Table 3), to locate mutations where necessary (see below).

Isolation and manipulation of nucleic acids

The isolation of genomic DNA and total RNA, as well as Southern and Northern blot analysis, was carried out as described previously (Etxebeste *et al*., 2008). DNA probes for Southern blot analysis were prepared by PCR amplification of coding regions of the corresponding gene (DIG Labelled Kit) with appropriate primers (Table 3) and genomic DNA of reference strain FGSC26. DNA probes for Northern blot analysis were obtained by PCR amplification of genomic DNA with the appropriate primers for each gene (see Table 3). Labelling of the probes was performed using Roche radioactive labelling kit. The Northern blot protocol used was essentially as described (Etxebeste *et al*., 2008), using hybridization solution (1% BSA, 1 mM EDTA, 0.5 M NaPO4, pH = 7.2 and 7% SDS; Church and Gilbert, 1984). Hybridizations were performed at 55°C for at least 18 h, and the filters were washed twice with a 2% SSC/0.1% SDS solution at 55°C, and if required, once with a 0.2% SSC/0.1% SDS solution at 55°C. Filters were exposed to radioactivity-sensitive films.

Generation of null, tagged and overexpression strains of FlbE

The null mutant of *flbE* was obtained by transforming TN02A3 with a DNA fragment containing 5′ and 3′ flanking regions of the ORF on either side of the auxotrophic marker *pyrG* of *A. fumigatus* (see Fig. S2). GFP- or Cherry-Red-labelled strains of *flbE* were obtained as described by Yang *et al*. (2004). All complemented strain carries a single homologous insertion.

In order to carry out bimolecular fluorescence experiments, FlbB and FlbE were each tagged with separate halves of YFP. The YFP^N and the YFP^C were fused to FlbB and FlbE respectively. To create YFP^N fusion construct of FlbB, a 3.2 kb fragment of *flbB* (starting from ATG) was amplified from genomic DNA, with the primers flbB-YFPsense and flbB-YFP antisense and cloned at the AscI and PacI sites into pYH01, containing *pyrG* from *A. fumigatus* (Takeshita *et al*., 2008), obtaining pAG101. The same approach was taken to produce YFP^C fusion of FlbE: a 1.5 kb fragment of *flbE* (starting from ATG) was amplified from genomic DNA, with the primers flbE-YFPsense and flbE-YFP antisense, and cloned using the same digestions into pYH102 (Takeshita *et al*., 2008), yielding pAG102. The XhoI–XhoI fragment from pAG102 was cloned into the corresponding sites of pBS-pyroA (contains *pyroA* from *A. fumigatus*, a kind gift from B. Oakley), yielding pAG103. pAG101 and pAG103 plasmids were then co-transformed into TN02A3 (Nayak *et al*., 2006). Transformants were culture in liquid MMA with 1% ethanol, in order to induce YFP-tagged protein expression.

Overexpression strains were constructed using plasmid pALC-pyroA*. This plasmid was obtained from plasmid pGPD, which contains the promoter and terminator regions *gpdA*, as well as a truncated form of *pyroA* (M.A. Peñalva, unpublished). The original promoter was eliminated by digestion with Asp718 and EcoRI, and the *alcA*, promoter (amplified by PCR) subsequently inserted at the same restriction sites. *alcA(p)::flbE* expressing plasmid was obtained by cloning *flbE* (PCR amplified with oligonucleotides *flbE*over sens and *flbE*over antis; see Table 3) into the EcoRI site of pALC-pyroA*. The plasmid was then transformed into TN02A3, Δ*flbE* and Δ*flbB* strains (Etxebeste *et al*., 2008).

Microscopy

Solid medium cultures were observed with a Nikon SMZ800 binocular microscope. Liquid medium cultures were observed with a Nikon Optiphot microscope under phase-contrast optics. Photographs were recorded with a Nikon AFX-DX camera. Hyphal descriptions and dimensions correspond to a minimum of 500 individual hyphae contained in a minimum of 50 separate photographic records.

Fluorescence images were obtained from *in vivo* cultures at 37°C with a DMI 6000B Leica microscope, with a 63× Plan Apo 1.4 N.A. oil immersion lens (Leica), illuminated with a 100 W mercury lamp and fitted with GFP (excitation 470 nm; emission 525 nm), Txred (excitation 562 nm; emission 624 nm), BGR (excitation 494 nm; emission 530 nm) and D (excitation 355 nm; emission 470 nm) filters, for GFP, Cherry-Red, YFP and DAPI fluorescence staining respectively.

In order to associate protein localization to different cytoskeletal networks (Araújo-Bazán *et al*., 2008), GFP-labelled strains were cultivated in liquid MMA for 16 h, and then transferred to medium containing Latrunculin B (Calbiochem, 100 μM) or Benomyl (Aldrich; 2.4 μg ml^{-1}). After 15 min, images were taken before transfer strains again to liquid MMA. Studies aimed at evaluating the dependency of protein localization on energy metabolism were carried out in the

same fashion using exposures to sodium azide (15 mM) and NaF (15 mM) for 5 min before transfer to liquid MMA (Peñalva, 2005; Araújo-Bazán *et al*., 2008).

Western blot analysis

Aspergillus nidulans was cultivated for 18 h in fermentation medium (Orejas *et al*., 1995), and filtered through two layers of Miracloth (Calbiochem), squeezed to eliminate excess liquid, frozen in dry ice and freeze-dried overnight. Protein extraction was carried out as previously described (Fernández-Martinez *et al*., 2003) and 50 g loaded into wells in 10% polyacrylamide gel. After electrophoretic separation, protein bands were electrotransferred onto nitrocellulose filters and later exposed to Roche anti-GFP mouse monoclonal antibody cocktail (1/1000) or, mouse anti-actin antibody (ICN Biomedical) 1/5000 for standard estimation of protein. Peroxidase-conjugated anti-mouse IgG immunoglobin (1/4000) (Jackson) was used as secondary antibody and development reagent.

Acknowledgements

The authors gratefully acknowledge technical assistance by M. Azcona and C. Falker. E.A.E. thanks Ministerio de Educación y Ciencia for support through Grant BFU2006-04185. U.U. thanks Ministerio de Educación y Ciencia for Grant BFU2004-03499/BMC and UPV/EHU for Grant GIU05/36. A.G. was a contract researcher under the research programme of Gipuzkoako Foru Aldundia/Diputación Foral de Gipuzkoa and Eusko Jaurlaritza/Gobierno Vasco, O.E. received a doctoral grant from UPV/EHU and was a contract researcher under CIC nanoGUNE, and E.H.-G. was a contract researcher under the research programme of Gipuzkoako Foru Aldundia/Diputación Foral de Gipuzkoa. The work was also supported by the Max-Planck-Institute for Terrestrial Microbiology, Marburg, Germany.

References

Adams, T.H., Wieser, J.K., and Yu, J.H. (1998) Asexual sporulation in *Aspergillus nidulans*. *Microbiol Mol Biol Rev* **62:** 35–54.

Aguirre, J. (1993) Spatial and temporal controls of the *Aspergillus brlA* developmental regulatory gene. *Mol Microbiol* **8:** 211–218.

Araújo-Bazán, L., Peñalva, M.A., and Espeso, E.A. (2008) Preferential localization of the endocytic internalization machinery to hyphal tips underlies polarization of the actin cytoskeleton in *Aspergillus nidulans*. *Mol Microbiol* **67:** 891–905.

Bartnicki-Garcia, S., Bartnicki, D.D., Gierz, G., Lopez-Franco, R., and Bracker, C.E. (1995) Evidence that Spitzenkörper behavior determines the shape of a fungal hypha: a test of the hyphoid model. *Exp Mycol* **19:** 153–159.

Bernreiter, A., Ramon, A., Fernández-Martinez, J., Berger, H., Araújo-Bazán, L., Espeso, E.A., *et al.* (2007) Nuclear export of the transcription factor NirA is a regulatory checkpoint for nitrate induction in *Aspergillus nidulans*. *Mol Cell Biol* **27:** 791–802.

Butnick, N.Z., Yager, L.N., Kurtz, M.B., and Champe, S.P. (1984) Genetic analysis of mutants of *Aspergillus nidulans* blocked at an early stage of sporulation. *J Bacteriol* **160:** 541–545.

Chang, Y.C., and Timberlake, W.E. (1993) Identification of *Aspergillus brlA* response elements (BREs) by genetic selection in yeast. *Genetics* **133:** 29–38.

Church, G.M., and Gilbert, W. (1984) Genomic sequencing. *Proc Natl Acad Sci USA* **81:** 1991–1995.

Etxebeste, O., Ni, M., Garzia, A., Kwon, N.J., Fischer, R., Yu, J.H., *et al.* (2008) Basic-zipper-type transcription factor FlbB controls asexual development in *Aspergillus nidulans*. *Eukaryot Cell* **7:** 38–48.

Fernández-Martinez, J., Brown, C.V., Diez, E., Tilburn, J., Arst, H.N., Peñalva, M.A., and Espeso, E.A. (2003) Overlap of nuclear localisation signal and specific DNA-binding residues within the zinc finger domain of PacC. *J Mol Biol* **334:** 667–684.

Fischer, R., and Kües, U. (2006) Asexual sporulation in mycelial fungi. In *The Mycota*, *Vol. I: Growth, Differentiation and Sexuality.* Kües, U., and Fischer, R. (eds). Berlin: Springer-Verlag, pp. 263–292.

Girbardt, M. (1957) Der Spitzenkörper von Polystictus versicolor (L.). *Planta* **50:** 47–59.

Horio, T., and Oakley, B.R. (2005) The role of microtubules in rapid hyphal tip growth of *Aspergillus nidulans*. *Mol Biol Cell* **16:** 918–926.

Kafer, E. (1965) Origins of translocations in *Aspergillus nidulans*. *Genetics* **52:** 217–232.

Law, D.J., and Timberlake, W.E. (1980) Developmental regulation of laccase levels in *Aspergillus nidulans*. *J Bacteriol* **144:** 509–517.

Lee, B.N., and Adams, T.H. (1994a) The *Aspergillus nidulans fluG* gene is required for production of an extracellular developmental signal and is related to prokaryotic glutamine synthetase I. *Genes Dev* **8:** 641–651.

Lee, B.N., and Adams, T.H. (1994b) Overexpression of *flbA*, an early regulator of *Aspergillus* asexual sporulation, leads to activation of *brlA* and premature initiation of development. *Mol Microbiol* **14:** 323–334.

Nayak, T., Szewczyk, E., Oakley, C.E., Osmani, A., Ukil, L., Murray, S.L., *et al.* (2006) A versatile and efficient gene-targeting system for *Aspergillus nidulans*. *Genetics* **172:** 1557–1566.

Orejas, M., Espeso, E.A., Tilburn, J., Sarkar, S., Arst, H.N., and Peñalva, M.A. (1995) Activation of the *Aspergillus* PacC transcription factor in response to alkaline ambient pH requires proteolysis of the carboxy-terminal moiety. *Genes Dev* **9:** 1622–1632.

Osherov, N., Mathew, J., and May, G.S. (2000) Polarity-defective mutants of *Aspergillus nidulans*. *Fungal Genet Biol* **31:** 181–188.

Peñalva, M.A. (2005) Tracing the endocytic pathway of *Aspergillus nidulans* with FM4-64. *Fungal Genet Biol* **42:** 963–975.

Polley, S.D., and Caddick, M.X. (1996) Molecular characterisation of meaB, a novel gene affecting nitrogen metabolite repression in *Aspergillus nidulans*. *FEBS Lett* **388:** 200–205.

Pontecorvo, G., Roper, J.A., Hemmons, L.M., McDonald,

K.D., and Bufton, A.W. (1953) The genetics of *Aspergillus nidulans*. *Adv Genet* **5:** 141–238.
Seo, J.A., Guan, Y., and Yu, J.H. (2006) FluG-dependent asexual development in *Aspergillus nidulans* occurs via derepression. *Genetics* **172:** 1535–1544.
Skromne, I., Sanchez, O., and Aguirre, J. (1995) Starvation stress modulates the expression of the *Aspergillus nidulans brlA* regulatory gene. *Microbiology* **141:** 21–28.
Steinberg, G. (2007a) Preparing the way: fungal motors in microtubule organization. *Trends Microbiol* **15:** 14–21.
Steinberg, G. (2007b) Hyphal growth: a tale of motors, lipids, and the Spitzenkörper. *Eukaryot Cell* **6:** 351–360.
Stinnett, S.M., Espeso, E.A., Cobeno, L., Araújo-Bazán, L., and Calvo, A.M. (2007) *Aspergillus nidulans* VeA subcellular localization is dependent on the importin alpha carrier and on light. *Mol Microbiol* **63:** 242–255.
Stringer, M.A., Dean, R.A., Sewall, T.C., and Timberlake, W.E. (1991) Rodletless, a new *Aspergillus* developmental mutant induced by directed gene inactivation. *Genes Dev* **5:** 1161–1171.
Taheri-Talesh, N., Horio, T., Araújo-Bazán, L., Dou, X., Espeso, E.A., Peñalva, M.A., *et al.* (2008) The tip growth apparatus of *Aspergillus nidulans*. *Mol Biol Cell* **19:** 1439–1449.
Takeshita, N., Higashitsuji, Y., Konzack, S., and Fischer, R. (2008) Apical sterol-rich membranes are essential for localizing cell end markers that determine growth directionality in the filamentous fungus *Aspergillus nidulans*. *Mol Biol Cell* **19:** 339–351.
Tilburn, J., Scazzocchio, C., Taylor, G.G., Zabicky-Zissman, J.H., Lockington, R.A., and Davies, R.W. (1983) Transformation by integration in *Aspergillus nidulans*. *Gene* **26:** 205–221.
Upshall, A.B., Giddings, B., and Mortimore, I.D. (1977) The use of benlate for distinguishing between haploid an diploid strains of *Aspergillus nidulans* and *Aspergillus terreus*. *J Gen Microbiol* **100:** 413–418.
Waring, R.B., May, G.S., and Morris, N.R. (1989) Characterization of an inducible expression system in *Aspergillus nidulans* using *alcA* and tubulincoding genes. *Gene* **79:** 119–130.
Wieser, J., and Adams, T.H. (1995) *flbD* encodes a Myb-like DNA-binding protein that coordinates initiation of *Aspergillus nidulans* conidiophore development. *Genes Dev* **9:** 491–502.
Wieser, J., Lee, B.N., Fondon, J., 3rd, and Adams, T.H. (1994) Genetic requirements for initiating asexual development in *Aspergillus nidulans*. *Curr Genet* **27:** 62–69.
Yang, L., Ukil, L., Osmani, A., Nahm, F., Davies, J., De Souza, C.P.C., *et al.* (2004) Rapid production of gene replacement constructs and generation of a green fluorescent protein-tagged centromeric marker in *Aspergillus nidulans*. *Eukaryot Cell* **3:** 1359–1362.
Yu, J.H. (2006) Heterotrimeric G protein signaling and RGSs in *Aspergillus nidulans*. *J Microbiol* **44:** 145–154.
Yu, J.H., Wieser, J., and Adams, T.H. (1996) The *Aspergillus* FlbA RGS domain protein antagonizes G protein signaling to block proliferation and allow development. *EMBO J* **15:** 5184–5190.
Yu, J.H., Mah, J.H., and Seo, J.A. (2006) Growth and developmental control in the model and pathogenic *Aspergilli*. *Eukaryot Cell* **5:** 1577–1584.

Supporting information

Additional supporting information may be found in the online version of this article.

Please note: Wiley-Blackwell are not responsible for the content or functionality of any supporting materials supplied by the authors. Any queries (other than missing material) should be directed to the corresponding author for the article.

